# Phosphorus Species Recovery Dependence on Acid Type during Dissolution-Precipitation Treatment of the Incineration Ash of Chicken Manure

Shigeru SUGIYAMA[1]*, En-Hong LIU[2,3], Kenta IMANISHI[2], Naohiro SHIMODA[1], Masahiro KATOH[1], and Jhy-Chern LIU[3]

[1]*Department of Applied Chemistry, Graduate School of Technology, Industrial and Social Sciences, Tokushima University, Minamijosanjima, Tokushima-shi, Tokushima 770-8506, Japan*

[2]*Department of Chemical Science and Technology, Tokushima University, Minamijosanjima, Tokushima-shi, Tokushima 770-8506, Japan*

[3]*Department of Chemical Engineering, National Taiwan University of Science and Technology, 43 Keelung Road, Section 4, Taipei 106, Taiwan*

In order to utilize chicken manure as a source of phosphorus, we used dissolution-precipitation treatment to recover phosphorus from the incineration ash of chicken manure (IACM), which was used as fuel to power a boiler. In order to recover useful phosphorus-containing solids from IACM, it was dissolved into aqueous solutions of either nitric acid, hydrochloric acid, or sulfuric acid to elute phosphorus together with various component elements, followed by the use of aqueous $NH_3$ to form a precipitate containing phosphorus. In using nitric acid and hydrochloric acid, calcium phosphate species such as calcium hydroxyapatite ($Ca_{10}(PO_4)_6(OH)_2$) and monetite ($CaHPO_4$) were obtained following the precipitation treatment. By contrast, the use of sulfuric acid resulted in the precipitation of magnesium ammonium phosphate (MAP) species such as struvite ($MgNH_4PO_4 \cdot 6H_2O$) and dittmarite ($MgNH_4PO_4 \cdot H_2O$). Both the calcium phosphate and MAP species can be used as a slow-acting fertilizer containing phosphorus, while the MAP species could be simultaneously used as a slow-acting fertilizer containing nitrogen. It is noteworthy that the calcium phosphate species obtained in the present study was equivalent to phosphate rock, which is widely used as a raw material in phosphorous-based industries, and the natural sources of this material could be depleted in the near future. Though IACM has not been used effectively until now, this new resource shows promise as s viable alternative to the dwindling supply of the natural sources of phosphorus.

## Introduction

Phosphorus is an element that is essential for living organisms, and it is widely used in food production as a main component in fertilizers and pesticides (Nakasaki *et al*., 2014). The demand for phosphorus is increasing and economically extractable phosphorus-containing reserves are expected to be exhausted within 50-100 years (Rolewics *et al*., 2016; Lee and Kim, 2017). In addition, phosphate rock reserves are geopolitically unbalanced, because known deposits are found predominately in Morocco, Russia, China and the USA, while Western Europe and India are almost completely dependent on importation (Cordell *et al*., 2009; Ashley *et al*., 2011). For Japan, the recovery of phosphorus from waste is very important because Japan has no natural phosphorus resources. (Kaikake *et al*., 2009).

Tokushima Prefecture is one of the largest production areas of *Jidori* (free range chickens) in Japan. However, it is well known that the processing of chicken manure is now overwhelming chicken farmers. To promote the effective utilization of chicken manure, a project to use chicken manure as fuel for boiler power generation was started in 2015 in the Tokushima Prefecture. The power generation itself is working well, but the incineration ash of chicken manure (IACM) emitted from boilers can only be used as fertilizer (Sugiyama *et al*., 2019). If phosphate rock equivalents and multifunctional phosphorus-containing compounds could be recovered from IACM, this would greatly expand the utilization of IACM that now is only used as fertilizer.

Previous studies of phosphorus recovery from waste materials have examined extraction from sewage sludge, sewage sludge ash, and IACM. The methods for extracting phosphorus from these wastes include electro-kinetic (Sturm *et al*., 2010), thermo-chemical (Adam *et al*., 2009), bioleaching and accumulation (Zimmermann and Dott, 2009), and wet chemical methods using acid leaching (Biplob Kumar Biswas *et al*., 2009; Donatello *et al*., 2010) and acid-base leaching with subsequent precipitation (Kaikake *et al*., 2009; Levlin *et al*., 2005; Petzet *et al*., 2011, Sugiyama *et al*., 2019). In the present study, the wet chemical methods were investigated due to the low efficiency and long processing times required for the other methods.

The development of phosphorus-recovery technologies has generally focused on the separation of

heavy metals from the phosphorus and on the conversion of phosphorus either into a plant-available form for reuse as fertilizer or into a raw material for the phosphorus-industry. The wet chemical methods can be classified as acid and alkaline dissolution techniques. In acidic dissolution, phosphorus and some of the metals are simultaneously dissolved. Therefore, after acidic dissolution, the dissolved phosphorus must be separated from the heavy metal ions in order to create a phosphorus recovery product with a low level of heavy metal content. Fortunately, the IACM used in the present study contained low levels of heavy metals compared with the levels detected in sewage sludge ash (Levlin et al., 2005; Oshita et al., 2003; Kaikake et al., 2009).

The purpose of the present study was to examine the recovery of phosphorus from IACM. In order to recover the phosphorus, a combination of acid-dissolution and alkali-precipitation was employed. Three types of acid, hydrochloric, nitric, and sulfuric, were used for the dissolution of the IACM. Ammonia was added to adjust the pH in order to obtain precipitation that was expected to produce calcium phosphates and magnesium ammonium phosphates. Calcium phosphates such as tricalcium phosphate ($Ca_3(PO_4)_2$), monetite ($CaHPO_4$) and calcium hydroxyapatite ($Ca_{10}(PO_4)_6(OH)_2$) are phosphate rock equivalents that can be used for the production of various phosphorus-containing materials and can be used as a slow-acting phosphorus fertilizer. Magnesium ammonium phosphate (MAP) species such as struvite ($MgNH_4PO_4·6H_2O$) and dittmarite ($MgNH_4PO_4·H_2O$) can be used as an advanced fertilizer that simultaneously provides phosphorus and nitrogen. In our previous paper (Sugiyama et al., 2019), phosphate rock equivalents were easily recovered from IACM using a combination of acid-dissolution with $HNO_3$ and alkali-precipitation with aqueous $NH_3$.

As shown above, our project for recovering phosphorus from unused solid resources via the wet chemical method combined with precipitation using ammonia was focused on recovering phosphorus as phosphate rock equivalents that could be directly used in industrial processes and in high-performance fertilizers that are directly used in agriculture. Most of the other phosphorus recovery have focused on eluting phosphorus and/or increasing the concentration of phosphorus from unused solid resources. In those cases, the recovered phosphorus contains so many impurities that it cannot be reused in the phosphorus-related plants currently in operation, and it is best to use it as a low-quality fertilizer that adds very little value. If we could recover high-purity phosphate rock equivalents and high-performance fertilizers as in our project, we will be able to obtain high-value-added phosphorus-containing products. This is a feature of our project.

## 1. Experimental

A power generation plant in the Tokushima Prefecture that used IACM as fuel (Sugiyama et al., 2019) provided the discharged ash, which was used as supplied due to a moisture content less than 1%. Along with major elements such as P, Ca, and Mg that were the focus in this study, major constituent elements such as Fe, Al, and Mn were measured by inductively coupled plasma atomic emission spectroscopy (ICP-AEC, SPS3520UV, SII Nanotechnology Inc.), and the results are shown in **Table 1**.

In the present study, in order to obtain calcium phosphates and various MAP species from IACM, first, IACM was dissolved in acid and filtered (dissolution process). Then, aqueous $NH_3$ was added to the filtrate to precipitate the phosphorus-containing solids (precipitation process). The error due to ICP was estimated to be within 1.2% at each measurement point. The conditions of IACM changes daily, but in this study, the error between samples was estimated to fall within 20%.

In the dissolution process, the dissolution behaviors of phosphorus and various cations from IACM were examined via the batch method. An aqueous acidic solution (100 mL) of either $HNO_3$, HCl, or $H_2SO_4$ was added to a 200 mL flask. Into this solution, IACM (1.0 g) previously sieved using a 355-μm mesh was added, followed by stirring at 130 rpm and 298 K in a constant-temperature water bath. After a scheduled amount of stirring time, the solution was filtered using filter paper (4 μm of pore size) and a membrane filter (0.45 μm of pore size), and the resultant filtrate was then analyzed by ICP-AES. The phosphorus-leaching efficiency (PLE) was then calculated using Eq. (1).

$$PLE\ (\%) = C_F/C_A \times 100 \qquad (1)$$

In Eq. (1), $C_F$ and $C_A$ refer to the concentration of P given as mmol/100 mL in the filtrate and in the ash, respectively. Corresponding equations were also used to calculate the leaching efficiencies for Ca and Mg.

In the precipitation process, aqueous $NH_3$ was added into the filtrate obtained in the dissolution process to adjust the pH to 6.0, 7.0 and 8.0 using a magnetic-stirrer at 200 rpm for 30 min. The solution was then filtered using a paper filter (pore size of 4 μm) and a membrane filter (pore size of 0.45 μm). The precipitates thus obtained were dried in an oven for 1 day and their crystalline structure was analyzed via X-ray diffraction (XRD; SmartLab/RA/INP/DX, Rigaku Co.) spectroscopy using monochromatized Cu Kα radiation (45 kV, 150 mA). The concentrations of the various cations in the filtrate obtained in the precipitation process were analyzed via ICP-AES. Phosphorus precipitation efficiency (PPE) was calculated using Eq. (2).

$$PPE\ (\%) = (1 - C_P/C_D) \times 100 \qquad (2)$$

In Eq. (2), $C_P$ and $C_D$ refer to the concentration of P given as mmol/100 mL in the filtrate obtained in the precipitation and in the dissolution processes, respectively. Corresponding equations were also used to calculate the precipitation efficiencies for Ca and Mg.

**Table 1** Content of the incineration ash of chicken manure as estimated by ICP-AES

| Content [mmol/g] | | | | | |
|---|---|---|---|---|---|
| P | Ca | Mg | Fe | Al | Mn |
| 1.68 | 7.51 | 1.01 | 0.05 | 0.11 | 0.03 |

The addition of ammonia to the acidic solution obtained in the dissolution process was simulated to observe the effect on the precipitation of calcium phosphates and magnesium ammonium phosphate via application of the geochemical aquatic modeling program, PHREEQC, interactive version 3.1.7-9213 (Song *et al.*, 2015). In the simulation, the following precipitation model and thermodynamic solubility products (Ksp) were adopted for brushite (CaHPO$_4$·2H$_2$O) (Liu *et al.*, 2017), monetite (CaHPO$_4$) (Johnsson *et al.*, 1992), calcium hydroxyapatite (Ca$_{10}$(PO$_4$)$_6$(OH)$_2$) (Kumar *et al.*, 2004; Moreno *et al.*, 1968), calcium phosphate (Ca$_3$(PO$_4$)$_2$) (Gregory *et al.*, 1974), newberyte (MgHPO$_4$·3H$_2$O) (Musvoto *et al.*, 2000), magnesium ammonium phosphate (MAP: MgNH$_4$PO$_4$) (Bhuiyan *et al.*, 2007) and bobierrite (Mg$_3$(PO$_4$)$_2$·8H$_2$O) (Musvoto *et al.*, 2000), respectively.

$$Ca^{2+}+HPO_4^{2-}+H_2O \leftrightarrow CaHPO_4 \cdot 2H_2O \quad \log Ksp = -6.6$$
$$Ca^{2+}+HPO_4^{2-} \leftrightarrow CaHPO_4 \quad \log Ksp = -6.8$$
$$5Ca^{2+}+3PO_4^{3-}+OH^- \leftrightarrow Ca_{10}(PO_4)_6(OH)_2 \quad \log Ksp = -117$$
$$3Ca^{2+}+2PO_4^{3-} \leftrightarrow Ca_3(PO_4)_2 \quad \log Ksp = -28.9$$
$$Mg^{2+}+HPO_4^{2-}+3H_2O \leftrightarrow MgHPO_4 \cdot 3H_2O \quad \log Ksp = -5.8$$
$$Mg^{2+}+PO_4^{3-}+NH_4^+ \leftrightarrow MgNH_4PO_4 \quad \log Ksp = -13.4$$
$$3Mg^{2+}+2PO_4^{3-}+8H_2O \leftrightarrow Mg_3(PO_4)_2 \cdot 8H_2O \quad \log Ksp = -25.2$$

## 2. Results and Discussion

### 2.1 Dissolution Process Using HNO$_3$, HCl, or H$_2$SO$_4$

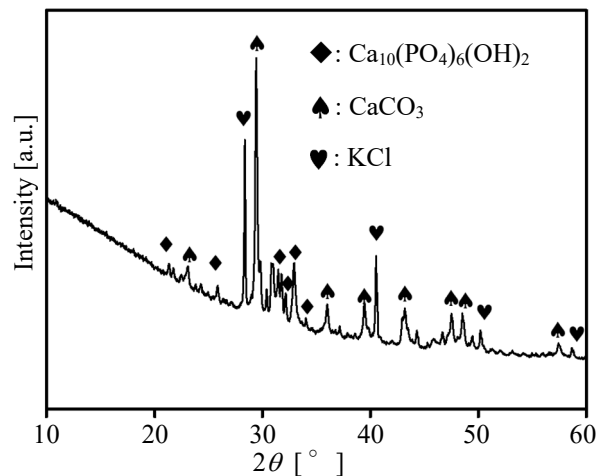**Figure 1** shows the XRD pattern of IACM used in the present study.



**Fig. 1** XRD patterns of the incineration ash of chicken manure

The IACM contained calcium hydroxyapatite (Ca$_{10}$(PO$_4$)$_6$(OH)$_2$; PDF 00-055-0592), calcite (CaCO$_3$; PDF 01-086-2334) and potassium chloride (KCl; PDF 00-004-0587). It should be noted that both the content (Table 1) and the XRD patterns (Figure 1) were different from those reported in our previous paper (Sugiyama *et al.*, 2019), which indicates that the nature of the IACM was strongly influenced by both the time and the place for the collection of the ash, as described in the Experimental section.
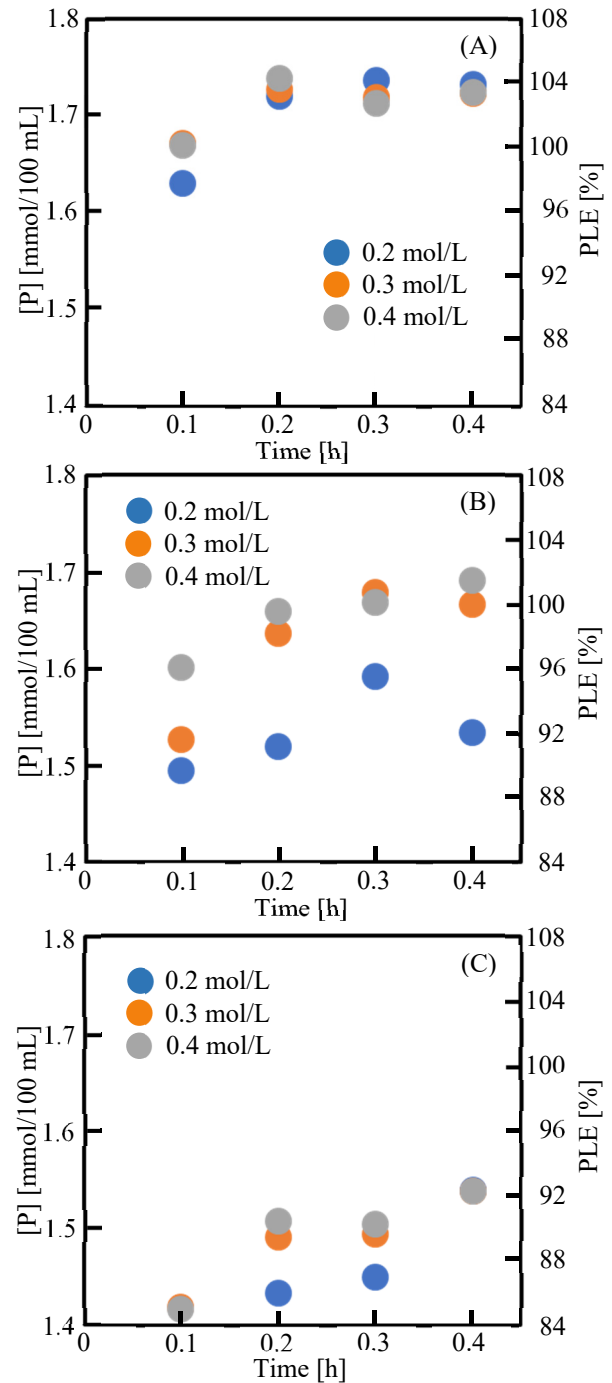


**Fig. 2** The elution behaviors of P from IACM (1.0 g) using various concentrations of (A) HNO$_3$, (B) HCl and (C) H$_2$SO$_4$

**Figures 2 (A)**, **(B)**, and **(C)** show the elution behaviors of P from IACM (1.0 g) in a dissolution process using 0.2, 0.3, and 0.4 mol/L of $HNO_3$, HCl, or $H_2SO_4$ solutions (each 100 mL) with stirring times of up to 0.4 h. The vertical axis of Figure 2 shows the amount of P (mmol) eluted from the IACM in those acidic solutions (100 mL). In these Figures, the phosphorus leaching efficiencies (PLE) were often above 100%, probably due to the non-uniformity of the IACM, as described above. The most available elution of P from IACM was observed via elution with $HNO_3$ (Figure 2 (A)). The elution of P reached maximum after 0.2 h of stirring time and was insensitive to the concentration of $HNO_3$. When 0.2 mol/L of HCl was used, the elution of P was insufficient with a maximum that was smaller than that obtained using $HNO_3$ (Figure 2 (B)). It is noteworthy that after filtration the filtrate shown in Figure 2 was used in the subsequent precipitation process. In the precipitation process, aqueous $NH_3$ was added to the filtrate, which could have caused an undesired formation of chloride species in the use of HCl. In contrast to the elution behavior of P when using $HNO_3$ and HCl, the use of $H_2SO_4$ showed an insufficient elution of P (Figure 2 (C)). Since there was no great difference between the elution using $HNO_3$ or HCl and that using $H_2SO_4$ (**Table 2**), the suppression of the elution using $H_2SO_4$ could have been influenced by factors other than pH. In the filtrate obtained after the filtration of the solution used to obtain the results shown in Figure 2 (C), an excess amount of sulfate ion was present together with the eluted phosphate ion. Sulfate ion is known to strongly interact with the calcium ion eluted from IACM (Kordlaghari and Rowell, 2006), which means that in addition to phosphate rock equivalent, it may be possible to obtain another solid rather than calcium phosphates during the precipitation process.

**Table 2** Change in pH corresponding to Figure 2

| Time | HNO$_3$ 0 h | HNO$_3$ 0.4 h | HCl 0 h | HCl 0.4 h | H$_2$SO$_4$ 0 h | H$_2$SO$_4$ 0.4 h |
|---|---|---|---|---|---|---|
| 0.2* | 0.81 | 1.57 | 0.76 | 0.95 | 0.84 | 1.77 |
| 0.3* | 0.64 | 0.99 | 0.61 | 0.74 | 0.67 | 1.07 |
| 0.4* | 0.52 | 0.74 | 0.50 | 0.60 | 0.55 | 0.79 |

\* Concentration (mol/L) of each acid

When the residue obtained in the filtrate after the filtration of the resultant solution shown in Figure 2 (C) was analyzed via XRD, gypsum ($CaSO_4 \cdot 2H_2O$; PDF 01-076-8726) was detected, as shown in **Figure 3**. Therefore, since IACM was covered with sparingly-soluble gypsum during the dissolution process using $H_2SO_4$, the PLE was evidently suppressed as shown in Figure 2 (C). **Table 3** shows the concentration and the leaching efficiencies of Ca and Mg eluted at 0.3 h using 0.4 mol/L of $HNO_3$, HCl, or $H_2SO_4$. Although both Ca and Mg were key elements, as described in the following section, these two elements could be separated by the proper use of acid. The concentrations and the leaching efficiency of Mg in the eluates were insensitive to those

three acids, while the concentration of Ca during the use of $H_2SO_4$ was evidently lower than that when using either $HNO_3$ or HCl, which indicated that most of the Ca had disappeared from the eluate when using $H_2SO_4$ and was precipitated as gypsum, as shown in Figure 2.
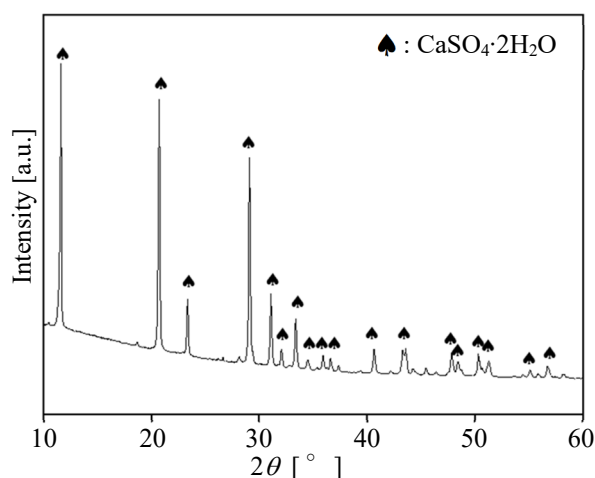


**Fig. 3** XRD pattern for the solid residue in the filtrate after the filtration of the solution shown in Figure 2 (C)

**Table 3** Concentration and leaching efficiencies (LE) of calcium and magnesium eluted at 0.3 h using 0.4 mol/L of acids

|  | Ca Conc.[1] | Ca LE [%] | Mg Conc.[1] | Mg LE [%] |
|---|---|---|---|---|
| HNO$_3$ | 7.55 | 100.5 | 0.82 | 81.2 |
| HCl | 5.74 | 76.4 | 0.82 | 81.2 |
| H$_2$SO$_4$ | 2.15 | 28.2 | 0.82 | 81.2 |

[1] mmol/100 mL.

## 2.2 Precipitation Process Using Aqueous NH$_3$

In order to precipitate a phosphorous-containing solid from the filtrate obtained in the dissolution process at 0.3 h using 0.4 mol/L of $HNO_3$, HCl, or $H_2SO_4$, aqueous $NH_3$ was added to each filtrate to adjust the solution pH to 6.0, 7.0, and 8.0. **Table 4** summarizes the corresponding precipitation efficiencies of P, Ca, and Mg. For the three acids, the precipitation efficiencies of P, Ca, and Mg were increased with an increase in pH. Approximately 70% of the precipitation efficiency of P from $HNO_3$ and HCl was obtained at pH 6.0, while approximately 94% and 99% were obtained at pH 7.0 and pH 8.0, respectively. For $H_2SO_4$, the precipitation efficiency of P was evidently lower than other acids. A precipitation efficiency of P at 20.9% was obtained at pH 6.0, which increased to 62.3% as the pH increased to 7.0, and increased to 85.4% at pH 8.0. For Ca, the precipitation efficiency from elution with $HNO_3$ was the highest. A precipitation efficiency of 33.2% was obtained at pH 6.0, which was increased to 42.9 and 50.7% at pH

7.0 and 8.0, respectively. The precipitation efficiency of Ca from elution with HCl was lower than that from HNO$_3$, but the rate was increased from 11.8% to 33.3% as the pH was increased from 6.0 to 8.0. The lowest precipitation efficiency of Ca was obtained during elution with H$_2$SO$_4$, 5.5% at pH 6.0, but was increased to 7.0 and 24.6% at pH 7.0 and 8.0, respectively. For Mg, the precipitation efficiency was highest from elution with H$_2$SO$_4$ and increased from 0.0% at pH 6.0 to 80.0% and 91.7% at pH 7.0 and pH 8.0, respectively. The precipitation efficiency of Mg from elution with HNO$_3$ was 0.71% at pH 6.0, which was increased to 28.0% at pH 7.0 and to 32.8% at pH 8.0. A Mg precipitation efficiency of 19.2% was obtained from elution with HCl at pH 6.0, which was increased to 17.6% and 19.2% at pH 7.0 and 8.0, respectively. Based on these results, the chemical species that make up the precipitation are expected to be strongly influenced by the type of acid used in the dissolution process.

**Table 4** Precipitation efficiencies of P, Ca, and Mg

| HNO$_3$ | Conc.[1] | Precipitation efficiency [%] | | |
| | | pH = 8.0 | pH = 7.0 | pH = 6.0 |
| --- | --- | --- | --- | --- |
| P | 1.75 | 99.8 | 94.8 | 72.0 |
| Ca | 7.55 | 50.7 | 42.9 | 33.2 |
| Mg | 0.82 | 32.8 | 28.0 | 0.71 |
| HCl | Conc.[1] | Precipitation efficiency [%] | | |
| | | pH = 8.0 | pH = 7.0 | pH = 6.0 |
| P | 1.75 | 99.3 | 94.1 | 68.3 |
| Ca | 5.74 | 33.3 | 26.4 | 11.8 |
| Mg | 0.82 | 19.2 | 17.6 | 0.0 |
| H$_2$SO$_4$ | Conc.[1] | Precipitation efficiency [%] | | |
| | | pH = 8.0 | pH = 7.0 | pH = 6.0 |
| P | 1.50 | 85.4 | 62.3 | 20.9 |
| Ca | 2.15 | 24.6 | 7.0 | 5.5 |
| Mg | 0.82 | 91.7 | 80.0 | 0.0 |

[1] mmol/100 mL in each filtrate obtained after the dissolution process.

**Figure 4 (A)** features an XRD pattern of the precipitation from filtrate using HNO$_3$. With adjustment of the pH to 7.0 and 8.0, calcium hydroxyapatite (Ca$_{10}$(PO$_4$)$_6$(OH)$_2$) was detected as a main component, which then became monetite (CaHPO$_4$; PDF 01-070-0360) at pH = 6.0. The XRD patterns of the precipitation from the filtrate eluted with HCl (**Figure 4 (B)**) also detected ammonium chloride (NH$_4$Cl; PDF 01-072-2378) with either calcium hydroxyapatite or monetite, but simple washing with water eliminated the ammonium chloride. Since calcium hydroxyapatite and monetite are the main components in phosphate rock, a phosphate rock equivalent could be obtained from IACM by using HNO$_3$ and HCl as an acidic eluate in the dissolution process. It is noteworthy that calcium phosphate species were not detected by XRD using the precipitation from the filtrate eluted with H$_2$SO$_4$.

Although the weight of the precipitation obtained at pH = 6.0 was too small to analyze using XRD, the XRD patterns of the precipitation obtained at pH = 7 and 8

showed the formation of MAP species such as struvite (MgNH$_4$PO$_4$·6H$_2$O; PDF 01-077-2303) and dittmarite (MgNH$_4$PO$_4$·H$_2$O; PDF 00-036-1491) (**Figure 4 (C)**). Therefore, XRD revealed that phosphate rock equivalent or MAP may be selectively precipitated by controlling the acid type used in the process.
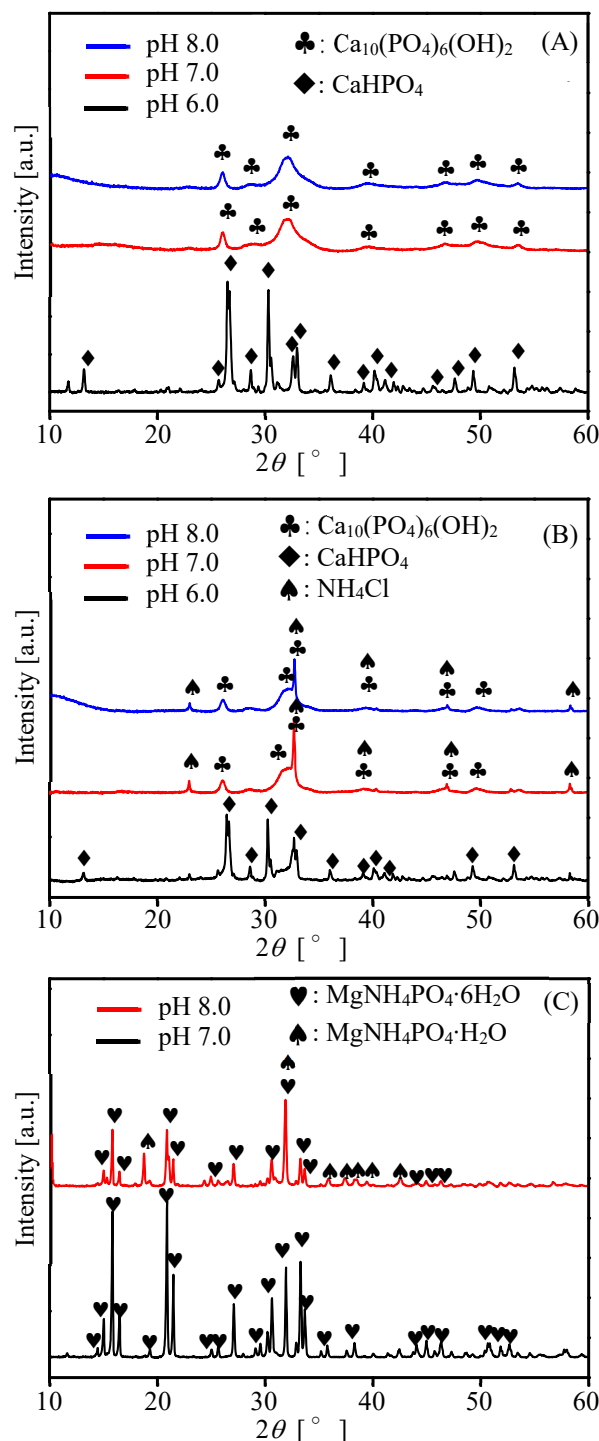


**Fig. 4** XRD patterns of the precipitates from the filtrate using (A) HNO$_3$, (B) HCl, or (C) H$_2$SO$_4$

As shown in **Table 5**, from 1.0 g of IACM, approximately 0.25-0.28 g of the precipitate was recovered when either $HNO_3$ or $HCl$ were used, while 0.10-0.18 g was recovered when using $H_2SO_4$. Regardless of the acid type, it was evident that a greater amount of precipitation was recovered at higher pH. Elementary analysis of the precipitation was carried out since Table 4 revealed that each precipitation seemed to contain both Ca and Mg, in contrast to the results shown in Figure 4. Therefore, each precipitation was completely dissolved in aq. HCl and analyzed using ICP-AES. As shown in Table 5, the precipitation obtained when using $HNO_3$ and HCl as an eluate continued to contain a small amount of Mg. In the case of $H_2SO_4$, the atomic ratio of Ca/Mg was strongly influenced by the solution pH.

**Table 5** Weight of the recovered precipitation and the content of P, Ca and Mg in the precipitation

| Acid | pH | R.W.[1] [g] | P | Ca | Mg |
|------|-----|------|------|------|------|
|      |     |      | [mmol/g] | | |
| $HNO_3$ | 8.0 | 0.285 | 4.974 | 6.415 | 0.276 |
|      | 7.0 | 0.284 | 4.823 | 5.475 | 0.160 |
|      | 6.0 | 0.250 | 5.574 | 5.163 | 0.067 |
| HCl  | 8.0 | 0.281 | 4.974 | 6.163 | 0.206 |
|      | 7.0 | 0.279 | 6.194 | 7.353 | 0.198 |
|      | 6.0 | 0.257 | 6.329 | 7.043 | 0.067 |
| $H_2SO_4$ | 8.0 | 0.180 | 5.439 | 2.217 | 3.417 |
|      | 7.0 | 0.108 | 5.100 | 0.837 | 3.878 |

[1] Recovered weight of each precipitation from 1.0 g of IACM.

Based on the PHREEQC simulation for the effects of the addition of ammonia to the acidic solution obtained in the dissolution process using $HNO_3$ and HCl, calcium hydroxyapatite was the only phase predicted to form at pH 5.0-9.0. In contrast, monetite was detected both using $HNO_3$ and HCl at pH 6.0, as shown in Figures 4 (A) and (B), respectively. The discrepancy between the experimental and simulation results was due to a PHREEQC simulation built on thermodynamic equilibrium. However, other factors such as reaction time, kinetics of the reaction, and other factors could affect the experimental results as well. Under high pH conditions, unstable forms of calcium phosphate, such as brushite ($CaHPO_4 \cdot 2H_2O$) and monetite ($CaHPO_4$) may transform into amorphous calcium phosphate very quickly and then become HAP after a considerably long period (Liu *et al*, 2001). The results of XRD at pH 6 in Figure 4 were obtained from the precipitate formed at pH 6 by adding ammonia to the filtrate after the dissolution process, followed by stirring for 30 minutes. After stirring for 30 minutes, the mixture was allowed to stand for 4 days, which confirmed that the reaction time had great influence on the precipitation. As shown in **Figures 5 (A) and (B)** for $HNO_3$ and HCl dissolution, respectively, both XRD results showed that monetite was transformed into calcium hydroxyapatite, brushite, octacalcium phosphate (OCP; $Ca_8H_2(PO_4)_6 \cdot 5H_2O$) and other phosphate species. Therefore, the reason that only

monetite was obtained in Figures 4 (A) and (B) at pH 6, contrary to the results of the PHREEQC simulation, was that the equilibrium was not reached due to the short treatment time.
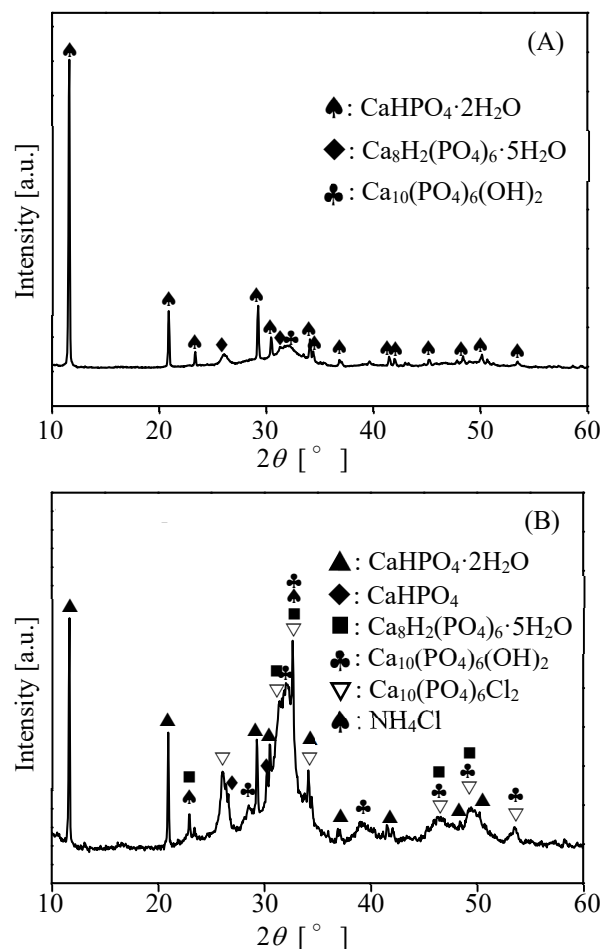


**Fig. 5** XRD patterns of the precipitates from the filtrate using (A) $HNO_3$ and (B) HCl but after standing for 4 days

**Table 6** lists the PHREEQC simulation results when using $H_2SO_4$. Calcium hydroxyapatite was excluded in the modelling since the $SO_4^{2-}$ could have inhibited the formation of calcium hydroxyapatite (Toyama *et al*, 2013). Based on the PHREEQC simulation, amorphous calcium phosphate and MAP were predicted to form at pH 7.0 and 8.0. Figure 4 (C) shows formation of the MAP species but not the calcium phosphate species, while the results listed Table 5 show the formation of calcium phosphate species together with MAP species. Therefore, these results together with PHREEQC simulation results suggested the formation of amorphous calcium phosphate species together with MAP species after the addition of ammonia to the acidic solution obtained in the dissolution process using $H_2SO_4$. Similar results on the precipitation of amorphous calcium phosphate and the MAP species at pH 7.0 and 8.0 were also reported (Abbona *et al*., 1986).

**Table 6** Molar fraction (%) simulated using PHREEQC in using $H_2SO_4$

| pH | 5 | 6 | 7 | 8 | 9 |
|---|---|---|---|---|---|
| Monetite | 0 | 100 | 0 | 0 | 0 |
| $Ca_3(PO_4)_2$ | 0 | 0 | 77.6 | 70.5 | 71.5 |
| MAP | 0 | 0 | 22.4 | 29.5 | 28.5 |

## 2.3 Contamination in the precipitation

As shown in Table 5 and Figure 4, in addition to calcium phosphates and MAP, contamination not detected by XRD must have been present in the precipitation obtained after the addition of aqueous $NH_3$. Therefore, in order to promote crystal growth, some of the precipitates shown in Figure 4 were calcined at 1,073 K for 5 h and then analyzed using XRD (**Figure 6**). With the use of $HNO_3$ (**Figure 6 (A)**), the precipitate obtained at pH = 8 was converted from calcium hydroxyapatite to tricalcium phosphate ($Ca_3(PO_4)_2$; PDF 01-076-6031). This conversion was the same as that reported in our previous paper (Sugiyama *et al*., 2019) and is reasonable since calcium hydroxyapatite is known to convert to calcium phosphate at temperatures higher than 973 K (Sugiyama *et al*., 1998).
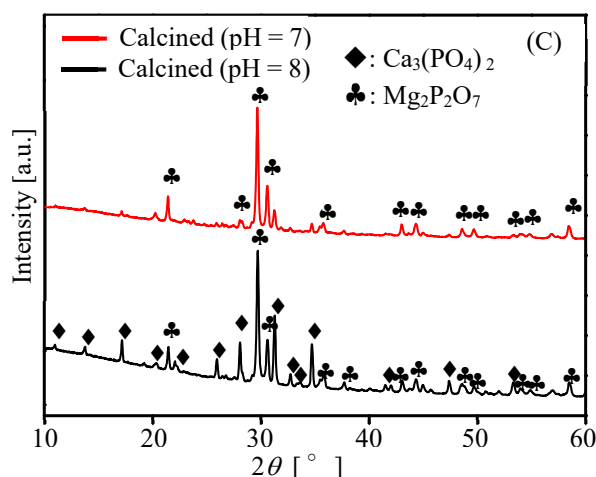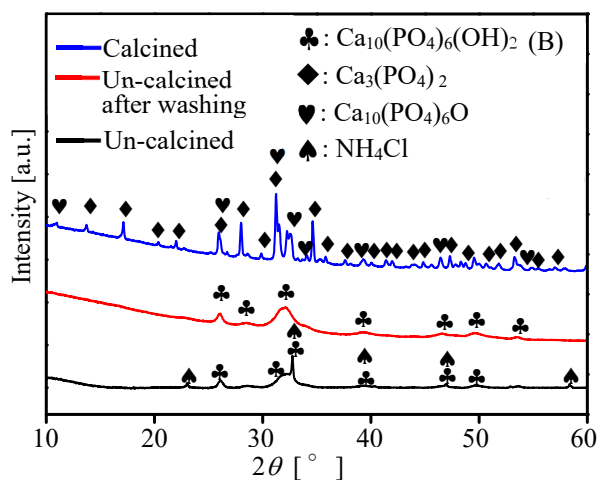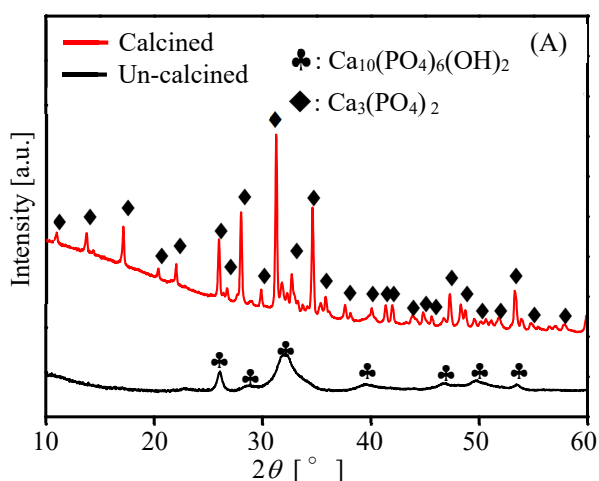
**Fig. 6** XRD patterns of samples obtained after calcination of the precipitations from the filtrate using (A) $HNO_3$, (B) HCl and (C) $H_2SO_4$

When HCl was used (**Figure 6 (B)**), $NH_4Cl$ was completely eliminated from the precipitate obtained at pH = 8 after washing with water, as previously mentioned. In contrast to Figure 5 (A), the precipitate was converted from calcium hydroxyapatite to tricalcium phosphate and $Ca_{10}(PO_4)_6O$ (PDF 01-089-6495). In these cases, magnesium-containing compounds were not detected since the content of magnesium was evidently lower than that of calcium, as shown in Table 5. Based on the XRD patterns of the solid samples obtained after the calcination of the precipitate via dissolution using $H_2SO_4$, magnesium pyro-phosphate ($Mg_2P_2O_7$; PDF 01-073-0535) was detected as the main peaks (**Figure 6 (C)**). As shown in Table 5 and Figure 6 (C), a neutral pH of ca. 7.0 seemed suitable for the preferential formation of magnesium pyro-phosphate.

Since MAP species such as struvite and dittmarite are already known to easily convert to magnesium pyro-phosphate at temperatures higher than 573K (Sugiyama *et al*., 2005), the detection of pyro-species is reasonable.

## Conclusions

In the present study, we selectively recovered calcium phosphate species as phosphate rock equivalents or magnesium ammonium phosphate as bifunctional fertilizers containing nitrogen and phosphorous from IACM using a dissolution-precipitation method that employed $HNO_3$, HCl and $H_2SO_4$ as eluates in the dissolution process.

## Acknowledgements

**Literature Cited**

Abbona, F., H. E. Lundager Madsen and R. Boistelle; "The Initial Phases of Calcium and Magnesium Phosphates Precipitated from Solutions of High to Medium Concentrations," *J. Cryst. Growth,* **74**, 581-590 (1986)

Adam, C., B. Peplinski, M. Michaelis, G. Kley and F.-G. Simon; "Thermochemical Treatment of Sewage Sludge Ashes for Phosphorus Recovery," *Waste Manage.*, **29**, 1122-1128 (2009)

Ashley, K., D. Cordell and D. Mavinic; "A Brief History of Phosphorus: from the Philosopher's Stone to Nutrient Recovery and Reuse," *Chemosphere*, **84**, 737-746 (2011)

Bhuiyan, M. I. H., D. S. Mavinic and R. D. Beckie; "A Solubility and Thermodynamic Study of Struvite," *Environ. Eng.*, **28**, 1015-1026 (2007)

Biswas, B. K., K. Inoue, H. Harada, K. Ohto and H. Kawakita; "Leaching of Phosphorus from Incinerated Sewage Sludge Ash by Means of Acid Extraction Followed by Adsorption on Orange Waste Gel," *J. Environ. Sci.*, **21**, 1753-1760 (2009)

Cordell, D., J.-O. Drangert and S. White; "The Story of Phosphorus: Global Food Security and Food for Thought" *Global Environ. Change,* **19**, 292-305 (2009)

Donatello, S., A. Freeman-Pask, M. Tyrer and C. R. Cheeseman; "Effect of Milling and Acid Washing on the Pozzolanic Activity of Incinerator Sewage Sludge Ash," *Cement Concr. Compos.*, **32**, 54-61 (2010)

Gregory, T. M., E. C. Moreno, J. M. Patel and W. E. Brown; "Solubility of β-Ca$_3$(PO$_4$)$_2$ in the System Ca(OH)$_2$-H$_3$PO$_4$-H$_2$O at 5, 15, 25, and 37℃," *J. Res. Natl. Bur. Stand. A, Phys. Chem.*, **78**, 667-674. (1974)

Johnsson, M. S. A. and G. H. Nancollas; "The Role of Brushite and Octacalcium Phosphate in Apatite Formation," *Crit. Rev. Oral Biol. Med.,* **3**, 61-82 (1992)

Kaikae, K., T. Sekito and Y. Dote; "Phosphate Recovery from Phosphorus-rich Solution Obtained from Chicken Manure Incineration Ash," *Waste Manage.*, **29**, 1084–1088 (2009)

Kordlaghari, M. P. and D. L. Rowell; "The Role og Gypsum in the Reactions of Phosphate with Soils," *Geoderma*, **132**, 105-115 (2006)

Kumar, R., K. H. Prakash, P. Cheang and K. A. Khor; "Temperature Driven Morphological Changes of Chemically Precipitated Hydroxyapatite Nanoparticles," *Langmuir*, **20**, 5196–5200 (2004)

Lee, M. and D.-J. Kim; "Identification of Phosphorus Forms in Sewage Sludge Ash during Acid Pre-treatment for Phosphorus Recovery by Chemical Fractionation and Spectroscopy," *J. Ind. Eng. Chem.*, **51**, 64-70 (2017)

Levlin, E., B. Hultman and M. Löwén; "Tvåstegslakning med Syra och Bas för Fosforutvinning ur Slam efter Superkritisk Vattenoxidation eller Förbränning," Svenskt Vatten AB, Stockholm, (2005)

Liu, C., Y. Huang, W. Shen and J. Cui; "Kinetics of Hydroxyapatite Precipitation at pH 10 to 11," *Biomater.*, **22**, 301-306 (2001)

Liu, Y. Z. Cheng, B. F. Branco and J. F. Marra; "Speciation and Mobility of Phosphate in the Eutrophic Ponds at Prospect Park, Brooklyn, New York, USA," *J. Geoscience Environ. Protect.*, **5**, 26-36 (2017)

Moreno, E. C., T. M. Gregory and W. E. Brown; "Preparation and Solubility of Hydroxyapatite," *J. Res. Nat. Bur. Stand., A. Phys. Chem.*, **72A**, 773-782 (1968)

Musvoto, E. V., M. C. Wentzel and G. A. Ekama; "Integrated Chemical–Physical Processes Modelling—II. Simulating Aeration Treatment of Anaerobic Digester Supernatants," *Water Res.*, **34**, 1868-1880 (2000)

Nakasaki, K.; "Phosphorus Recovery from Chicken Droppings Treated with Advanced Compositing Techniques," *Agriculture and Horticulture*, **89**, 524–530 (2014)

Oshita, K., M. Iwashita, M. Takaoka and N., Takeda; "Basic Study on Wet Extraction Process of Phosphorus from Sewage Sludge Ash," *Environ. Eng. Res.*, **40**, 395-404 (2003)

Petzet, S., B. Peplinski, S. Y. Bodkhe and P. Cornel; "Recovery of Phosphorus and Aluminium from Sewage Sludge Ash by a New Wet Chemical Elution Process (SESAL-Phos-recovery Process). *Water Sci. Technol.*, **64**, 693-699 (2011)

Rolewicz, M., P. Rusek, M. Mikos-Szymańska, B. Cichy and M. Dawidowicz; "Obtaining of Suspension Fertilizers from Incinerated Sewage Sludge Ashes (ISSA) by a Method of Solubilization of Phosphorus Compounds by Bacillus Megaterium Bacteria," *Waste Biomass Valor.*, **7**, 871–877 (2016)

Song, Y., F. Qian, Y. Gao, X, Huang, J. Wu and H. Yu; PHREEQC Program-based Simulation of Magnesium Phosphates Crystallization for Phosphorus Recovery," *Environ. Earth Sci.*, **73**, 5075-5084 (2015)

Sturm, G., H. Weigand, C. Marb, W. Weiβ and B. Huwe; "Electrokinetic Phosphorus Recovery from Packed Beds of Sewage Sludge Ash: Yield and Energy Demand," *J. Appl. Electrochem.*, **40**, 1069-1078 (2010)

Sugiyama, S., T. Minimi, T. Moriga, H. Hayashi and J. B. Moffat; "Calcium-lead Hydroxyapatites: Thermal and Structural Properties and the Oxidation of Methane," *J. Solid State Chem.*, **135**, 86–95 (1998)

Sugiyama, S., M. Yokoyama, H. Ishizuka, K.-I. Sotowa, T. Tomida and N. Shigemoto; "Removal of Aqueous Ammonium with Magnesium Phosphates Obtained from the Ammonium-elimination of Magnesium Ammonium Phosphate," *J. Colloid Interface. Sci*, **292**, 133–138 (2005)

Sugiyama, S., K. Wakisaka, K. Imanishi, M. Kurashina, N. Shimoda, M. Katoh and J.-C. Liu; "Recovery of Phosphate Rock Equivalents from Incineration Ash of Chicken Manure by Elution-precipitation Treatment," *J. Chem. Eng. Jpn*, **52**, 778-782 (2019)

Toyama, T., S. Kameda and N. Nihsimiya; "Synthesis of Sulfate-Ion-Substituted Hydroxyapatite from Amorphous Calcium Phosphate," Bioceram. Dev. Appl., S1, 011-013 (2013)

Zimmermann, J. and W. Dott; "Sequenced Bioleaching and Bioaccumulation of Phosphorus from Sludge Combustion – a New Way of Resource Reclaiming," *Adv. Mater. Res.,* (Zuerich, Switzerland), **71-73**, 625-628 (2009)